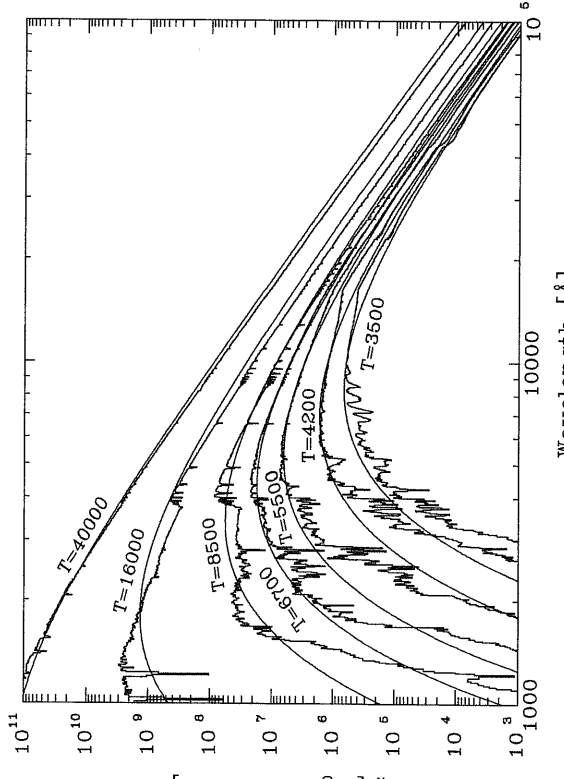


2 Stars: Basic Observations



In this chapter we examine some of the basic observed properties of stars—their spectra, temperatures, emitted power, and masses—and the relations between those properties. In Chapter 3, we proceed to a physical understanding of these observations.

2.1 Review of Blackbody Radiation

To a very rough, but quite useful, approximation, stars shine with the spectrum of a **blackbody**. The degree of similarity (but also the differences) between stellar and blackbody spectra can be seen in Fig. 2.1. Let us review the various descriptions and properties of blackbody radiation (which is often also called *thermal radiation*, or radiation having a *Planck spectrum*). A blackbody spectrum emerges from a system in which matter and radiation are in thermodynamic equilibrium. A fundamental result of quantum mechanics (and one that marked the beginning of the quantum era in 1900) is the exact functional form of this spectrum, which can be expressed in a number of ways.

The **energy density** of blackbody radiation, per frequency interval, is

$$(2.1) \quad u_\nu = \frac{8\pi\nu^2}{c^3} \frac{h\nu}{e^{h\nu/kT} - 1},$$

where ν is the frequency, c is the speed of light, h is Planck's constant, k is Boltzmann's constant, and T is the temperature in degrees Kelvin. Clearly, the first term has units of [time]/[length]³ and the second term has units of energy. In cgs units, u_ν is given in erg cm⁻³ Hz⁻¹.

Next, let us consider the flow of blackbody energy radiation (i.e., photons moving at speed c), in a particular direction inside a blackbody radiator. To obtain this so-called intensity, we take the derivative with respect to solid angle of the energy density and

Figure 2.1 Flux per wavelength interval emitted by different types of stars, at their “surfaces,” compared to blackbody curves of various temperatures. Each blackbody’s temperature is chosen to match the total power (integrated over all wavelengths) under the the corresponding stellar spectrum. The wavelength range shown is from the ultraviolet ($1000 \text{ \AA} = 0.1 \mu\text{m}$), through the optical range ($3200\text{--}10,000 \text{ \AA}$), and to the mid-infrared ($10^5 \text{ \AA} = 10 \mu\text{m}$). Data credit: R. Kurucz.

multiply by c (since multiplying a density by a velocity gives a flux, i.e., the amount passing through a unit area per unit time):

$$(2.2) \quad I_\nu = c \frac{du_\nu}{d\Omega},$$

where $d\Omega$ is the solid angle element. (For example, in spherical coordinates, $d\Omega = \sin\theta d\theta d\phi$.) Blackbody radiation is isotropic (i.e., the same in all directions), and hence the energy density per unit solid angle is

$$(2.3) \quad \frac{du_\nu}{d\Omega} = \frac{u_\nu}{4\pi}$$

(since the solid angle of a full sphere is 4π steradians). The intensity of blackbody radiation is therefore

$$(2.4) \quad I_\nu = \frac{c}{4\pi} u_\nu = \frac{2h\nu^3}{c^2} \frac{1}{e^{h\nu/kT} - 1} \equiv B_\nu.$$

In cgs, one can see the units now are erg s⁻¹ cm⁻² Hz⁻¹ steradian⁻¹. We have kept the product of units, s⁻¹ Hz⁻¹, even though they formally cancel out, to recall their different physical origins: one is the time interval over which we are measuring the amount of energy that flows through a unit area, and the other is the photon frequency interval over which we bin the spectral distribution. I_ν of a blackbody is often designated B_ν .

and

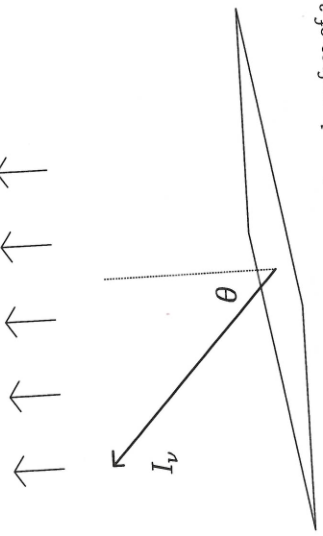


Figure 2.2. Illustration of the net flux emerging through surface of a blackbody, due to a beam with intensity I_v emerging at an angle θ to the perpendicular.

Now, let us find the net flow of energy that emerges from a unit area (small enough so that it can be presumed to be flat) on the outer surface of a blackbody (see Fig. 2.2). This is obtained by integrating I_v over solid angle on the half-sphere facing outward, with each I_v weighted by the cosine of the angle between the intensity and the perpendicular to the area. This **flux**, which is generally what one actually observes from stars and other astronomical sources, is thus

$$f_v = \int_{\theta=0}^{\pi/2} I_v \cos \theta d\Omega = I_v 2\pi \frac{1}{2} = \pi I_v = \frac{c}{4} u_v = \frac{2\pi h\nu^3}{c^2} \frac{1}{e^{h\nu/kT} - 1}. \quad (2.5)$$

The cgs units of this flux per frequency interval will thus be erg s⁻¹ cm⁻² Hz⁻¹.

The total power (i.e., the energy per unit time) radiated by a spherical, isotropically emitting, star of radius r_* is usually called its **luminosity**, and is just

$$L_v = f_v(r_*) 4\pi r_*^2, \quad (2.6)$$

with cgs units of erg s⁻¹ Hz⁻¹. Similarly, the flux that an observer at a distance d from the star will measure will be

$$f_v(d) = \frac{L_v}{4\pi d^2} = f_v(r_*) \frac{r_*^2}{d^2}.$$

It is often of interest to consider the above quantities integrated over all photon frequencies, and designated by

$$u = \int_0^\infty u_v dv, \quad I = \int_0^\infty I_v dv, \quad f = \int_0^\infty f_v dv, \quad L = \int_0^\infty L_v dv. \quad (2.8)$$

A case in point is the useful **Stefan-Boltzmann law**, which relates the total energy density and flux of a blackbody to its temperature:

$$u = \sigma T^4, \quad (2.9)$$

$$f = \frac{c}{4} a T^4 = \sigma T^4, \quad (2.10)$$

$$a = \frac{8\pi^5 k^4}{15c^3 h^3} = 7.6 \times 10^{-15} \text{ erg cm}^{-3} \text{ K}^{-4},$$

$$\sigma = \frac{c}{4} a = 5.7 \times 10^{-5} \text{ erg s}^{-1} \text{ cm}^{-2} \text{ K}^{-4}.$$

(Here and throughout this book, numbers are rounded off to two significant digits, except in some obvious cases where higher accuracies are warranted.)

Rather than considering energy density, intensity, flux, and luminosity per photon frequency interval, we can also look at these quantities per photon wavelength interval, where the wavelength is $\lambda = c/v$. To make the transformation, we recall that the energy in an interval must be the same, whether we measure it in wavelength or frequency, so,

$$B_\lambda d\lambda = B_v d\nu, \quad (2.11)$$

and hence

$$B_\lambda = B_v \left| \frac{d\nu}{d\lambda} \right| = B_v \frac{c}{\lambda^2} = \frac{2hc^2}{\lambda^5} \frac{1}{e^{hc/\lambda kT} - 1}. \quad (2.12)$$

Here the units are erg s⁻¹ cm⁻² steradian⁻¹, where we have separated the two length units (cm⁻² and cm⁻¹), since one is the unit area through which the radiation flux is passing, and the other is the wavelength interval over which we bin the radiation energy. Non-cgs units for the wavelength interval are common in astronomy. For example, flux per wavelength interval at visual wavelengths is often given in units of erg s⁻¹ cm⁻² Å⁻¹. An Å (called “angstrom”) is 10^{-8} cm.

The wavelength or frequency of the peak of a blackbody spectrum can be found by taking its derivative and equating to zero:

$$\frac{dB_\lambda}{d\nu} = 0, \quad (2.13)$$

or

$$\frac{dB_\lambda}{d\lambda} = 0, \quad (2.14)$$

which lead to the two forms of Wien’s law:

$$\lambda_{\max} T = 0.29 \text{ cm K} \quad (2.15)$$

and

$$h\nu_{\max} = 2.8 kT. \quad (2.16)$$

14 | Chapter 2

For example, the nearest star—the Sun—which radiates approximately like a blackbody at $T = 5800\text{ K}$, has a peak in B_λ at 5000 \AA , which is the wavelength of green light, in the middle of the visual regime. In fact, the eyesight of most animals on Earth apparently evolved to have the most sensitivity in the wavelength range within which the Sun emits the most energy. (No less important, this wavelength range also coincides with the transmission range of water vapor in the atmosphere.) Note that the frequency ν_{\max} where B_ν peaks is *not* the same as the frequency $\nu = c/\lambda_{\max}$ at which B_λ peaks. The two spectral distributions are different, because a constant-frequency interval $d\nu$ corresponds to a changing wavelength interval

$$(2.17) \quad d\lambda = \left| \frac{d\lambda}{d\nu} \right| d\nu = \frac{c}{\nu^2} d\nu.$$

that grows with wavelength (and falls with frequency).

Figure 2.1 shows blackbody spectral distributions for a variety of temperatures. The following features are important to note. First, the functions described above (μ_ν , B_ν , etc.) are determined uniquely by one parameter, the temperature. Second, far from their peak frequencies or wavelengths, the Planck blackbody spectra assume two simple forms, as can be easily verified by taking the appropriate limits in Eqs. 2.4 and 2.12. At frequencies ν much lower than the peak (i.e., at photon energies $h\nu \ll kT$),

$$(2.18) \quad B_\nu \approx \frac{2\nu^2}{c^2} kT$$

$$\text{or} \quad (2.19)$$

$$B_\lambda \approx 2ckT\lambda^{-4}.$$

This is called the **Rayleigh-Jeans side** of the thermal spectrum. At frequencies much higher than the peak (photon energies $h\nu \gg kT$) the blackbody spectrum falls off exponentially with frequency as

$$B_\nu \sim e^{-(h\nu/kT)},$$

or with decreasing wavelength as

$$B_\lambda \sim e^{-(hc/\lambda kT)}.$$

This is called the **Wien tail** of the distribution.

2.2 Measurement of Stellar Parameters

2.2.1 Distance

Distances to the nearest stars can be measured via **trigonometric parallax**. With current technology, about 100,000 stars have had their distances measured in this way. The motion

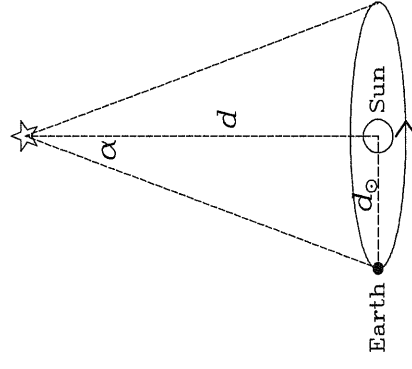


Figure 2.3 Schematic view of the apparent parallax motion of a nearby star, situated in the direction above the ecliptic plane, due to the Earth's circular orbit around the Sun.

of the Earth around the Sun produces an apparent movement on the sky of nearby stars, relative to more distant stars. Stars in the direction perpendicular to the plane of the Earth's orbit (called the *ecliptic plane*) will trace a circle on the sky in the course of a year (see Fig. 2.3), whereas stars in the directions of the ecliptic plane will trace on the sky a line segment that doubles back on itself. In other directions, stars will trace out an ellipse. The angular size of the semi-major axis of the ellipse will obviously be

$$(2.22) \quad \alpha = \frac{d_\odot}{d},$$

with d_\odot the Earth–Sun distance and d the distance to the star. (The subscript \odot marks properties of the Sun—distance, mass, radius, etc.). The distance d_\odot , which is also referred to as 1 astronomical unit (AU), is about $1.5 \times 10^8\text{ km}$. Parallax is actually used to define another unit of length, a parsec (pc). One pc is defined as the distance for which the parallax is 1 arcsecond (i.e., $1/3600$ of a degree of arc, or $\pi/(180 \times 3600)$ radian). Thus,

$$(2.23) \quad 1\text{ pc} = 2.1 \times 10^5\text{ AU} = 3.1 \times 10^{18}\text{ cm} = 3.3\text{ ly},$$

where we have also expressed a parsec in light years (ly), the distance light travels in vacuum during a year. A light year is

$$(2.24) \quad 1\text{ ly} = 365.25 \times 24 \times 3600 \times c = 3.15 \times 10^7\text{ s} \times 3 \times 10^{10}\text{ cm s}^{-1}.$$

It is convenient to remember that the number of seconds in a year is (by pure coincidence) close to $\pi \times 10^7$. The few nearest stars to the Solar System have distances of about 1 pc. Most of the stars visible to the naked eye are closer than 100 pc. At larger distances, convenient units are the kiloparsec (kpc; 10^3 pc), megaparsec (Mpc; 10^6 pc), and gigaparsec (Gpc; 10^9 pc).

16 | Chapter 2

Apart from the apparent motion of stars due to parallax, stars have real motions relative to each other, and hence relative to the Sun. Over human timescales, these real relative motions will generally appear on the sky to have constant velocity and direction. In practice, therefore, the parallax motion of nearby stars will often be superimposed on a linear proper motion, producing a curly or wavy trajectory on the sky.

2.2.2 Stellar Temperatures and Stellar Types

As we will see later on, the volume of every star has a range of temperatures, from millions of degrees Kelvin in its core to only thousands in the outer regions. However, the emitted spectrum of a star is largely determined by the temperature in the outermost “surface,” or spectrum of its **photosphere**. The photosphere can be roughly defined as the region from which photons are able to escape a star without further absorption or scattering (see Fig. 2.4). As we will see, the scattering and absorption probabilities can have a strong dependence on the wavelength of the photon, and therefore the depth of the base of the photosphere can be wavelength dependent. Material at the base of the photosphere emits approximately a Planck spectrum, which is then somewhat modified by the cooler, partly transparent, gas above it. By examining the emerging spectrum, one can then define various temperatures. The **color temperature** is the temperature of the Planck function with shape most closely matching the observed spectrum. For example, if we could identify the position of the peak of the spectrum, we could use Wien’s law to set the temperature. In practice, the peak will often be outside the wavelength range for which we have data, and furthermore it is a broad feature that is hard to identify, especially given the modifications by cold absorbing gas above the last scattering surface.

A more practical variant is to measure the ratio of fluxes at two different wavelengths, $f_{\lambda}(\lambda_1)/f_{\lambda}(\lambda_2)$, and to find the temperature of the blackbody that gives such a ratio. Such a ratio is, in effect, what one always means by color. For example, when we say that we detect a larger ratio of red photons to blue photons than we would from an object that we would call “white.” Color temperature can, of course, also be found by fitting the Planck spectrum to measurements at more than two wavelengths. Note that a color temperature cannot be found if all the measurements are well on the Rayleigh-Jeans (i.e., low-energy) side of the distribution. On that side the Planck spectrum has the same shape for all temperatures ($f_{\lambda} \propto \lambda^{-4}$ or $f_{\nu} \propto \nu^2$), and hence the ratio of fluxes at two wavelengths or frequencies will be the same, irrespective of temperature. In such a case we can only deduce that all our measurements are on the Rayleigh-Jeans side of a Planck spectrum, and we can set a lower limit on the temperature of the spectrum (see Problem 2).

Another kind of temperature can be associated with the photosphere of a star, by examining the absorption features at discrete wavelengths in the stellar spectrum. These absorptions are induced by atoms and molecules in the cooler, less dense, gas above the surface of last scattering. Photons with energies equal to those of individual quantum energy

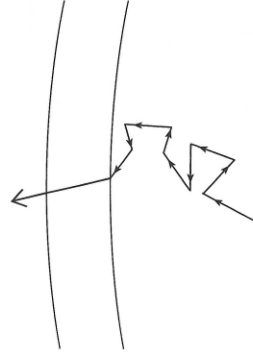


Figure 2.4 A photon inside a star is scattered many times until it reaches a radius from which it can escape. The last scattering surface defines the base of the photosphere of the star.

transitions of those atoms and molecules will be preferentially absorbed, and therefore depleted, from the light emerging from the photosphere of the star in the direction of a distant observer. The same atom or molecule, which will be excited to a higher energy level by absorbing a photon, can eventually decay radiatively and reemit a photon of the same energy. However, the reemitted photon will have a random direction, which will generally be different from the original direction toward the observer. Furthermore, the atom can undergo collisional deexcitation, in which it transfers its excitation energy to the other particles in the gas.

The wavelengths and strengths of the main absorption features, or absorption lines as they are often called, are primarily dependent on the level of ionization and excitation of the gas. The form of the absorption spectrum therefore reflects mainly the temperature of the photosphere, and only slightly the photosphere’s chemical composition, which is actually similar in most stars.

It is of particular relevance to recall the quantum structure of the hydrogen atom. Hydrogen is the simplest atom, and it is therefore useful for understanding how stellar absorption spectra are produced. Furthermore, most stars are composed primarily of hydrogen; 92% of the atoms, or 75% of the mass, is hydrogen. Almost all of the rest is helium, and the heavier elements contribute only trace amounts. In fact, this elemental makeup is typical of almost all astronomical objects and environments, other than rocky planets like the Earth and some special types of stars. The heavier elements, despite their low abundances in stars, still play important physical and observational roles, as we will see later on.

The n th energy level of the hydrogen atom ($n = 1$ is the ground state) is given by the Bohr formula,

$$E_n = -\frac{e^4 m_e}{2\hbar^2 n^2} = -13.6 \text{ eV} \frac{1}{n^2}, \quad (2.25)$$

where e is the electron charge in cgs units (e.s.u.), m_e is the electron mass, and \hbar is Planck’s constant divided by 2π . As one goes to higher n , the energy levels become more

that indicates the upper level of the transition. Thus, the Lyman series consists of all transitions to the $n = 1$ ground level:

$$\begin{aligned} \text{Ly}\alpha &: 2 \leftrightarrow 1, 1216 \text{ \AA} \\ \text{Ly}\beta &: 3 \leftrightarrow 1, 1025 \text{ \AA} \\ \text{Ly}\gamma &: 4 \leftrightarrow 1, 972 \text{ \AA} \\ \text{etc.,} & \\ &\text{up until the Lyman continuum,} \\ \text{Ly}_{\text{con}} &: \infty \leftrightarrow 1, < 911.5 \text{ \AA}. \end{aligned}$$

Similarly, the Balmer series includes all transitions between the $n = 2$ state and higher states:

$$\begin{aligned} \text{H}\alpha &: 3 \leftrightarrow 2, 6563 \text{ \AA} \\ \text{H}\beta &: 4 \leftrightarrow 2, 4861 \text{ \AA} \\ \text{H}\gamma &: 5 \leftrightarrow 2, 4340 \text{ \AA} \\ \text{etc.,} & \\ &\text{up until the Balmer continuum,} \\ \text{Ba}_{\text{con}} &: \infty \leftrightarrow 2, < 3646 \text{ \AA}. \end{aligned}$$

In the same way, the Paschen series, Brackett series, and Pfund series designate transitions where $n = 3, n = 4$, and $n = 5$, respectively, are the lower levels. The photon wavelengths of the Lyman series are in the ultraviolet (UV) region of the electromagnetic spectrum, and the Paschen, and higher, series occur at infrared (IR), and longer, wavelengths. The Balmer series is of particular interest to us here, as it occurs in the optical region of the spectrum, where Earth's atmosphere has a transmission window. The atmosphere is almost completely opaque to photons of wavelengths shorter than $\approx 3100 \text{ \AA}$, from ultraviolet through X-rays and γ -rays. At the infrared wavelengths longer than $10,000 \text{ \AA}$ ($1 \mu\text{m}$), there are only a few transmission "troughs," until one gets to millimeter (called microwave) wavelengths and longer, where the atmosphere is again transparent to radio-frequency electromagnetic radiation.

Early in the 20th century, before stellar physics was understood, stars were classified into a series of spectral types according to the types and strengths of the absorption lines appearing in their optical spectra. Figure 2.6 shows examples covering the range of spectral properties of most stars. Let us begin with A-type stars, the third from the top in the sequence shown (the meanings of the "5" and of the "V" after the "A" are explained below, and at the end of this chapter, respectively). Absorption in the hydrogen Balmer series is the most conspicuous feature in A-star spectra, starting with H α at 6563 \AA , proceeding up the series to shorter wavelengths, and to the sharp drop at the wavelength of the Balmer continuum at 3646 \AA . Moving up in the figure to B-type stars, the hydrogen lines become weaker, and some other lines, due to absorption by helium, appear. At the top of the sequence, O stars have only very weak hydrogen Balmer lines, and some additional weak lines due to singly ionized helium. Working back down along the sequence, in the so-called F-type stars, the Balmer lines are again weaker than in A stars, but additional lines appear,

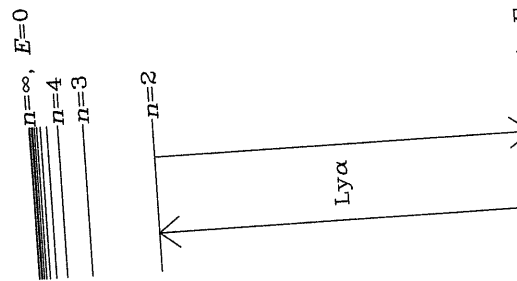


Figure 2.5 Energy levels of the hydrogen atom. Arrows indicate excitation from the ground state ($n = 1$) to the first excited energy level ($n = 2$), and deexcitation back to the ground state. Such excitation and deexcitation could be caused by, e.g., absorption by the atom of a Lyman- α photon, and subsequent spontaneous emission of a Lyman- α photon.

The wavelength¹ of a photon emitted or absorbed in a radiative transition between two levels will be

$$(2.27) \quad \lambda_{n_1, n_2} = \frac{hc}{E_{n_1, n_2}} = \frac{911.5 \text{ \AA}}{\frac{1}{n_1^2} - \frac{1}{n_2^2}}.$$

A glass tube in the laboratory filled with atomic hydrogen at low pressure, when excited by an electrical discharge, will radiate photons at the discrete wavelengths corresponding to all of these electronic energy transitions. Such a photon spectrum emitted to the thermal (i.e., blackbody) spectrum emitted from the thermal (i.e., blackbody) spectrum emitted by dense matter.

It is customary to group the different energy transitions of atomic hydrogen by a name identifying the lower energy level involved in the transition, combined with a Greek letter by dense matter.

¹ As customary in the astronomical research literature, wavelengths of atomic transitions are cited to four significant digits, as measured in air at standard temperature and pressure. Since the speed of light is smaller in air than in vacuum, the wavelengths in vacuum are longer by a factor equal to the index of refraction of air, 1.00028 for optical light.

the emerging beam, only Lyman-series photons, in the UV range, can therefore be absorbed out by the hydrogen atoms, while optical photons emerge through the photosphere unhindered by the hydrogen. The metal atoms, though they exist only in trace amounts, do have energy-level transitions corresponding to optical-wavelength photons, and hence these atoms have high probabilities for absorbing photons. Thus, they leave a strong imprint on the spectrum, despite their rarity compared with hydrogen.

Going to warmer stars, frequent collisions between atoms in the photosphere cause a nonnegligible fraction of the hydrogen atoms at any given time to be in the first excited ($n = 2$) energy state. Now the optical photons with the Balmer-transition energies can be absorbed out of the emerging light by the hydrogen atoms, thereby exciting the hydrogen atoms to higher levels, or ionizing them when the photon wavelengths are less than 3646 Å. In the hottest stars, the temperature in the photosphere is high enough that almost all of the hydrogen is ionized (as are the metal atoms). The photosphere then becomes transparent again to photons with the energies of the Balmer transitions, which have a low probability of being absorbed. Models of stellar atmospheres can be calculated, taking into account the detailed atomic physics and the passage of radiation through the gas, for a range of physical conditions, specifically the temperature. (In fact, the stellar spectra shown in Figs. 2.1 and 2.6 are theoretical models calculated by Kurucz.) Such theoretically calculated absorption spectra can be compared to the actual spectrum of a given stellar type, and thus the photospheric temperature can be accurately determined.

Generations of astronomy students have memorized the names of the stellar spectral types, ordered by decreasing temperature, with the mnemonic: "Oh Be A Fine Girl/Guy, Kiss Me!" There is a continuous transition in spectral properties between types, and astronomers quantify this by assigning, after the letter, a number between 0 and 9, with a larger number indicating a lower temperature. The Sun is a G2 star, and its spectrum is largely indistinguishable from that of any other normal star of this type. As we will see, all of the main physical properties (mass, radius, luminosity) of the stars sharing a common spectral classification are the same. For completeness, we note that the spectral sequence extends beyond M stars to two cooler classes, labeled L and T. Strictly speaking, members of these classes are not stars but *brown dwarfs*, objects intermediate between stars and giant planets in their properties. We return to brown dwarfs in section 4.2.3.4.

6600 and 8600 Å are mainly due to this molecule.

The names assigned to the different spectral types have a historical origin and no physical significance. However, the order in which they appear in Fig. 2.6 is one of temperature, with the hottest stars at the top and the coolest at the bottom. This is apparent at once by considering the colors of the stars. The O and B stars are clearly blue, with their spectra rising toward the shorter UV wavelengths of the peak of the blackbody spectrum. The A, F, and G stars become progressively "whiter." The K and M stars are clearly red, with their peak emission shifted to the infrared. The optical wavelength range shown probes the beginning of the Wien tail of the Planck function approximating these red stars.

Once the stars are ordered by temperature, the different absorption-line spectra can be understood as arising simply from the differences in the temperatures of the photospheres. In the cooler stars, the hydrogen atoms, which make up most of the cool gas above the last scattering surface, are almost all in their ground states. Among the photons in

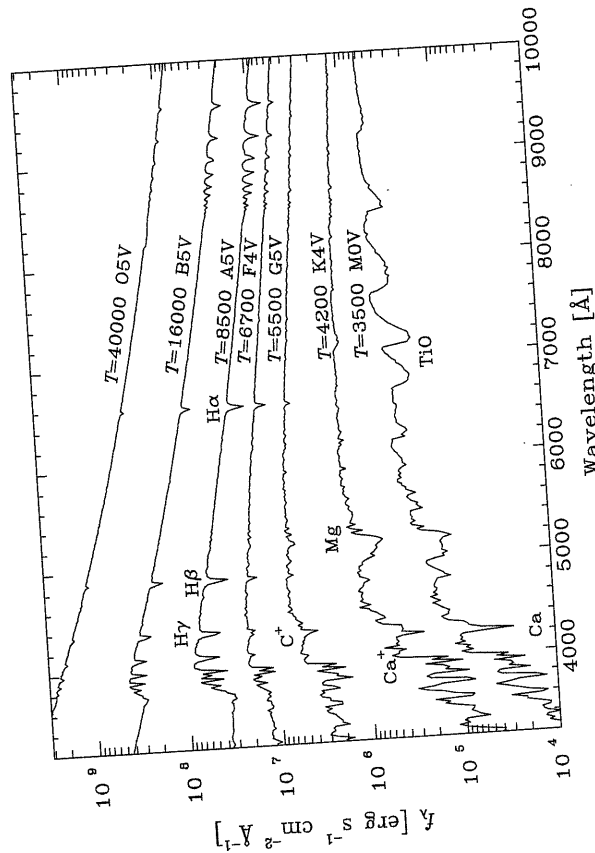


Figure 2.6 Zoom-in on the optical wavelength region of the stellar spectra shown in Fig. 2.1. The curves are labeled with their spectral types, in addition to the corresponding blackbody temperatures, which constitute the effective temperatures of the stars. Note the various labeled absorption features that appear and disappear as one goes from one spectral type to another. Data credit: R. Kurucz.

and are due to transitions in neutral and singly ionized light metals, mainly calcium, magnesium, and sodium. Progressing to G stars, the Balmer lines weaken further, while the absorptions due to metals become stronger. This trend continues in K stars where, in addition, molecular "bands" begin to appear. Such bands are actually numerous adjacent absorptions due to individual rotational, vibrational, and electronic quantum transitions of particular molecules, which have merged into broad absorption troughs. Finally, in M stars, at the bottom of the sequence, the molecular bands, notably due to TiO (titanium oxide), become prominent. The absorption bands seen in the M-star spectrum between 6600 and 8600 Å are mainly due to this molecule.

The names assigned to the different spectral types have a historical origin and no physical significance. However, the order in which they appear in Fig. 2.6 is one of temperature, with the hottest stars at the top and the coolest at the bottom. This is apparent at once by considering the colors of the stars. The O and B stars are clearly blue, with their spectra rising toward the shorter UV wavelengths of the peak of the blackbody spectrum. The A, F, and G stars become progressively "whiter." The K and M stars are clearly red, with their peak emission shifted to the infrared. The optical wavelength range shown probes the beginning of the Wien tail of the Planck function approximating these red stars.

Once the stars are ordered by temperature, the different absorption-line spectra can be understood as arising simply from the differences in the temperatures of the photospheres. In the cooler stars, the hydrogen atoms, which make up most of the cool gas above the last scattering surface, are almost all in their ground states. Among the photons in

2.2.3 Luminosity and Radius

For a star with known distance and measured flux, the luminosity is

$$L = f 4\pi d^2. \quad (2.28)$$

This luminosity, integrated over all wavelengths, is called the **bolometric luminosity**. If the temperature of the stellar photosphere is known, one can then derive the stellar radius, r_* , from

$$L = 4\pi r_*^2 \sigma T^4. \quad (2.29)$$

Alternatively, if L and r_* are known and one determines a temperature from this relation, then this temperature is called the **effective temperature**, T_E . The radius of the Sun is

$r_\odot = 7.0 \times 10^{10}$ cm. As will be explained in more detail in section 2.2.4, below, stars that are members of a particular type of binary system, called *double-lined spectroscopic eclipsing binaries*, can have their radii measured. Of order 100 stars currently have such radius measurements, which are accurate to a few percent or better. The radii of a few other nearby stars have been measured, in some cases to better than 1% accuracy, using interferometric observations.

2.2.4 Binary Systems and Measurements of Mass

A direct measurement of stellar mass is generally possible only in certain **binary** (i.e., double) or multiple star systems. A significant fraction of all stars are members of binary systems. (The Sun is likely an example of a single star.) Observationally, binary systems are classified into various types. **Visual binaries** are pairs of stars in which both members are resolved individually, and may be seen orbiting their common center of mass. In most cases, the separation between the members is so large that the orbital period is very long by human timescales. In **astrometric binaries**, one observes the minute periodic motion on the sky of one member, as it orbits the system's common center of mass, even if the companion is too faint to be seen. In **eclipsing binaries**, the orbital plane of a pair (which, in general, is spatially unresolved) is inclined enough (i.e., close enough to edge-on) to our line of sight that each of the members periodically eclipses the other. The presence of a binary will then be revealed if the light from the system is monitored as a function of time. During each orbital period, the brightness of the system will undergo two "dips" (see Fig. 2.7), each corresponding to the eclipse of one star by the other. The depth of the dips will depend on the relative sizes and luminosities of the two stars.

A **spectroscopic binary** is a spatially unresolved pair that is revealed as a binary by its spectrum. For example, the observed photospheric absorption spectrum may be the superposition of the spectra of two different types of stars. Alternatively, even if the members are of the same type, their orbital velocities, v , may cause large enough Doppler shifts, $\Delta\lambda/\lambda = v/c$, in the wavelengths of absorption, to produce distinct lines, with shifts that oscillate periodically during each orbit (see Fig. 2.8). Sometimes, one of the members may be too faint, or devoid of strong absorption lines, to be detectable in the combined spectrum, but its presence will still be revealed by the periodically changing Doppler shifts of the brighter star. In fact, this is the very method by which planets orbiting other stars have been discovered in recent years (see below).

To see how binaries sometimes allow stellar mass determination, let us review some aspects of the Keplerian two-body problem, in which two masses orbit their common center of mass in elliptical trajectories. For simplicity, let us consider only circular orbits. The center of mass of two spherical masses is at the point between them where

$$r_1 M_1 = r_2 M_2, \quad (2.30)$$

with M_1 and M_2 being the masses and r_1 and r_2 their respective distances to the center of mass (see Fig. 2.9, left). Thus, if $a = r_1 + r_2$ is the separation between the masses,

$$r_1 = \frac{M_2}{M_1 + M_2} a. \quad (2.31)$$

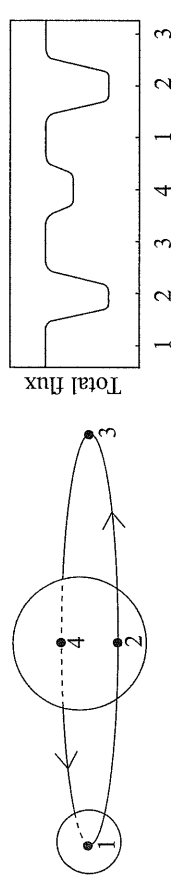


Figure 2.7 Schematic view of an eclipsing binary system (left), and its total brightness as a function of time (right). Numbers indicate the corresponding points on the orbit and in the so-called "light curve."

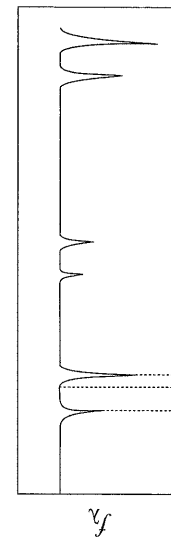


Figure 2.8 Schematic example of the spectrum of a double-lined spectroscopic binary. Each of the absorption lines in the spectrum appears twice, Doppler-shifted to longer and shorter wavelengths, respectively, as a result of the orbital motion of the binary members about their center of mass. During the orbital period, each absorption line oscillates back and forth about the restframe wavelength λ_0 .

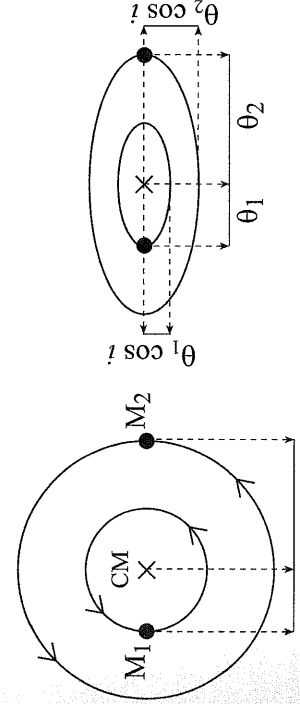


Figure 2.9 Left: A binary system, viewed pole-on, with its members in circular orbits with physical radii r_1 and r_2 around their common center of mass. Right: The appearance of the system when viewed as a visual binary, with the orbital plane inclined by an angle i to the line of sight, and orbital radii subtending angles on the sky θ_1 and θ_2 . The circular orbits now appear as ellipses, with minor axes foreshortened by $\cos i$.

$$\text{or} \quad r_1 = \frac{M_2}{M_1 + M_2} a \quad (2.32)$$

and

$$r_2 = \frac{M_1}{M_1 + M_2} a. \quad (2.33)$$